Superlattices and Microstructures 84 (2015) 144–153

Contents lists available at ScienceDirect

Superlattices and Microstructures

journal homepage: www.elsevier.com/locate/superlattices

Field emission property of ZnO nanowires prepared by ultrasonic spray pyrolysis

Myo Than Htay *, Yoshio Hashimoto

Department of Electrical and Electronic Engineering, Faculty of Engineering, Institute of Carbon Science and Technology, Shinshu University, 4-17-1 Wakasato, Nagano 380-8553, Japan

ARTICLE INFO

Article history:
Received 23 April 2015
Accepted 5 May 2015
Available online 14 May 2015

Keywords:
ZnO
Nanowire
Field emission
Oxide semiconductor
Ultrasonic spray pyrolysis

ABSTRACT

The field emission property of cold cathode emitters utilizing the ZnO nanowires with various conditions prepared by ultrasonic spray pyrolysis technique was discussed. It is found that the emission current was enhanced in the emitters having higher aspect ratio as well as smaller sheet resistance. Applying of post-annealing process, utilization of additional Mo back electrode in the cathode, and coating of Mo on the ZnO nanowires resulted in the improvement of the emission current and lowering the threshold voltage. A threshold voltage of about 5.5 V/μm to obtain 1.0 μA/cm^2 was achieved in the sample prepared at the growth temperatures varying continuously from 250 °C to 300 °C.

1. Introduction

Electron emission phenomenon observes at the surface of a solid material under an applied electric field in vacuum is well explained by the following expression known as Fowler–Nordheim (F–N) equation.

$$J = A\frac{(\beta E)^2}{\phi}\exp\left(\frac{-B\phi^{3/2}}{\beta E}\right) \quad (1)$$

Here, E represents an applied electric field, β is defined as a field enhancement factor which is depending on the morphological aspect ratio of the solid emitter, ϕ is the work function of the emission

* Corresponding author. Tel.: +81 (0)26 269 5241; fax: +81 (0)26 269 5220.
E-mail address: myoth@shinshu-u.ac.jp (M.T. Htay).

http://dx.doi.org/10.1016/j.spmi.2015.05.003
0749-6036/

surface, and A and B are the constants respectively [1,2]. This equation can be rearranged in the form as shown in Eq. (2), which is usually used for evaluating the β directly from the experimental measurement results.

$$\mathrm{Ln}\left(\frac{J}{E^2}\right) = \frac{-B\phi^{3/2}}{\beta}\cdot\frac{1}{E} + \mathrm{Ln}\left(\frac{A\beta^2}{\phi}\right) \tag{2}$$

From these equations it can be clearly understood that the emission current density J is depending on the applied electric field as well as the surface morphology of the emitter. Since one dimensional nano-structure such as nanowire has higher morphological aspect ratio than that of a flat surface thin film of the same material, β is significantly increase and it is possible to enhance the electron emission under an applied electric field even at room temperature by utilizing the structural advantage of nanowire. Accordingly, one dimensional material such as ZnO nanowires (abbreviated as ZNs) is know to be one of the promising materials for application in the cold cathode emitter due to its structural property of high aspect ratio [2–19]. In addition, ZNs has advantages in the environmental issue since it has no toxicity, no limitation in the resource, and it could be synthesized by various processes including non vacuum processes such as solution based reaction techniques and ultrasonic spray pyrolysis, in which only relatively low energy is required for the growth process [20–38]. Up to now, several researches have been focusing on the development of cold cathode field emission devices based on ZNs [2–19]. Recently, we also reported an economically viable synthesis technique of ZNs on a soda-lime glass (SLG) substrate utilizing ultrasonic spray pyrolysis (USP) [22–25]. In this paper, we focused on the field emission property of ZNs prepared by this USP technique in relation to various material parameters.

2. Experimental methods

The ZNs were prepared by utilizing our original USP system with some minor modifications, the detailed structure and processes of which were described in our previous reports [22–25,39]. In preparing the ZNs, a precursor solution containing zinc acetate dihydrate (abbreviated as ZA, Wako, 99%), indium (III) nitrate trihydrate (abbreviated as IN, Wako, 98%), and ammonium acetate (abbreviated as AA, Wako, 97%), which were dissolved in 1 L of deionized water by a specific molar ratio, was used. In our USP technique, ZNs with wurtzite crystal structure are usually obtained and the majority growth direction of one dimensional nanowire structure is observed to be along the [002] axis or c-axis. The details of material properties such as crystal structure, growth orientation, optical characteristics and etc. of the ZNs prepared by this USP technique were already reported in our previous reports [22–25]. For the field emission measurements, a device configuration as shown in Fig. 1 was used. A cathode emitter was formed by growing the ZNs emitter on the SLG substrate directly by USP. A self-assembled seeding layer with or without additional Mo back electrode was utilized as the back electrode of ZNs emitter. The details of self-assembled seeding layer were discussed in

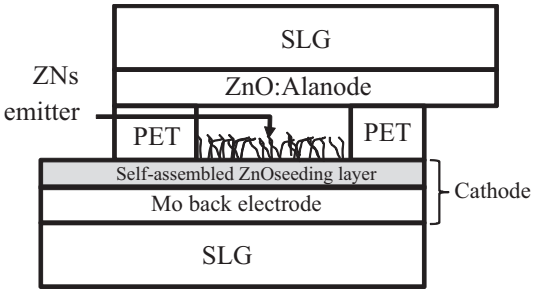

Fig. 1. The cross-sectional schematic of the device used for testing the field emission property. The Mo back electrode layer was not applied in some conditions, i.e., only the ZnO seedling layer was used as the cathode. The thickness of the films were not drawn to scale.

our previous reports [23,25]. A Poly-Ethylene Telephthalate (PET) film with 40 μm thickness was used to separate the ZNs emitter from the ZnO:Al transparent conductive anode film, which was deposited on the SLG substrate by RF magnetron sputtering. The area of active emission surface was 1.0 cm^2 and field emission measurements were carried out by applying a potential in the range of 0–600 V with 10 V steps between the two electrodes under the vacuum of 10^{-5} Torr. The morphology of ZNs was observed by a scanning electron microscope (FE-SEM, Hitachi, S-4100). The sheet resistance of ZNs

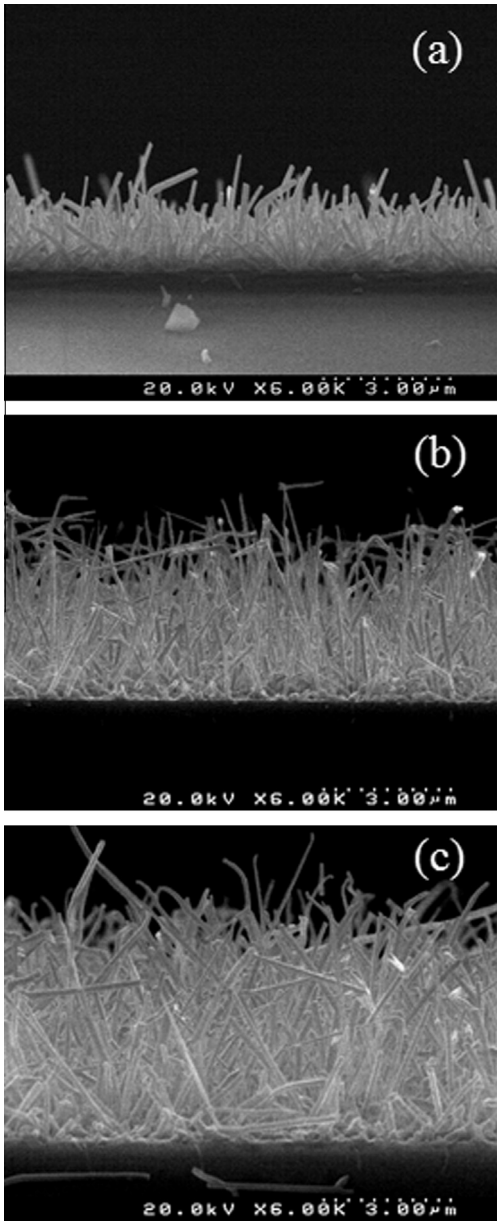

Fig. 2. The cross-sectional SEM images of the ZNs prepared at 300 °C for the growth periods of (a) 30 min, (b) 40 min, and (c) 50 min.

emitter grown on the self-assembled seeding layer was measured by a four-probe method (Kyowa Riken, K89PS, tips gap: 1 mm). To investigate the influence of morphological aspect ratio and/or material parameter such as resistance of the ZNs emitter on the field emission property, different types of ZNs prepared at different growth periods as well as temperatures as shown in Figs. 2 and 3 were used. The samples shown in Fig. 2(a)–(c) were prepared at the growth temperature of 300 °C for various growth periods of 30, 40, and 50 min utilizing the precursor solution containing solutes with the molar ratio of ZA:IN:AA = 0.18:0.018:0.9 respectively. The sample shown in Fig. 3(a) was prepared at the

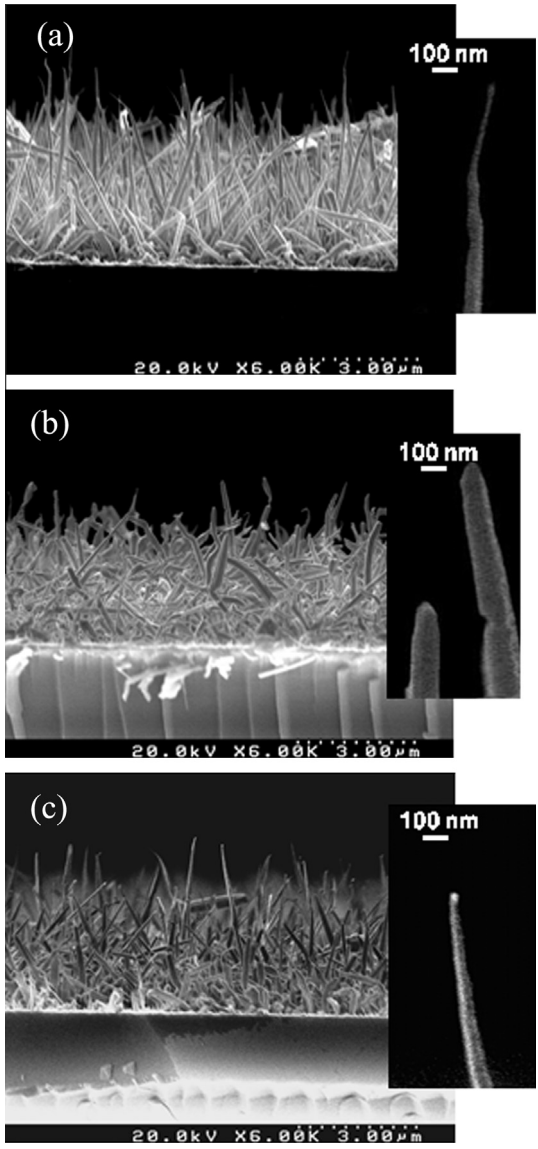

Fig. 3. The cross-sectional SEM images of the ZNs prepared at the growth temperatures of (a) 250 °C, (b) 300 °C, and (c) 250 °C to 300 °C continuous range utilizing precursor solution containing solutes with molar ratio of ZA:IN:AA = 0.18:0.036:0.9 respectively. The high resolution images showing the tip of ZNs are described on the right side of each corresponding cross-sectional image.

growth temperature of 250 °C and that of Fig. 3(b) was grown at 300 °C. For the sample shown in Fig. 3(c), the growth temperature was continuously increased from 250 °C to 300 °C during the growth period of 60 min utilizing the precursor solution containing solutes with molar ratio of ZA:IN:AA = 0.18:0.036:0.9. A post-annealing process of the sample prepared at 300 °C was conducted at 500 °C for 10 min under vacuum of 10^{-4} Torr in order to reduce the resistance of as-grown ZNs. The field emission property of the samples with or without an additional Mo back electrode was also measured to investigate the effect of sheet resistance of the whole cathode. In preparing the sample with Mo back electrode, RF magnetron sputtering of Mo layer was carried out before the NZs growth process. In the case of the sample containing ZNs emitter coated with Mo thin film, 2 nm thick Mo was sputtered after the formation of ZNs emitter.

3. Results and discussion

In Fig. 4, the result of field emission measurements of the samples shown in Fig. 2, the length (aspect ratio) of which were controlled by the growth period, is depicted. It is found that the lowest threshold voltage of about 6.3 V/μm to obtain 1.0 μA/cm^2 is achieved in the sample prepared at 300 °C for growth period of 40 min as shown in Fig. 4(b). For the samples prepared at 30 min and 50 min, larger thresholds such as 11.7 V/μm and 9.8 V/μm are obtained as shown in Fig. 4(a) and (c). By comparing the cross-sectional SEM images shown in Fig. 2, it is clearly observed that the average length of ZNs is increasing with the growth period. The average length of the sample prepared at 40 min is about 4 μm, which is twice to that of the sample prepared at 30 min. For the sample grown at 50 min, a longer average length of about 6 μm, which is about thrice to that of 30 min, is obtained. In addition, mutual interlacing between the nanowires of the sample prepared at 50 min is quite obvious compared to the other two. This result indicates that the variation of threshold voltage has good correlation to their corresponding length of ZNs in the samples prepared at 30 and 40 min. However, in the case of 50 min, the correlation is poor, i.e., the enhancement of emission is relatively lower although increasing factor of the length of ZNs is obviously higher. The increase of interlacing of nanowires in the sample prepared at 50 min could be the main reason that hindered the improvement of electron emission by screening effect so that trading off the benefit of increasing the length (enhancing of aspect ratio) of nanowires as shown in Fig. 4(c).

In Fig. 5, the result of field emission measurements of the samples shown in Fig. 3, the morphology of the tip of ZNs were controlled by changing the profile of growth temperatures, is plotted. The threshold voltages of the samples prepared at the constant growth temperatures of 300 °C and 250 °C are observed to be about 9.0 V/μm and 9.3 V/μm as shown in Fig. 5(a) and (b) respectively. For the sample shown in Fig. 3(c), which was prepared at the growth temperatures gradually varied from 250 °C to 300 °C during the growth period of 60 min, it is found that the threshold voltage is

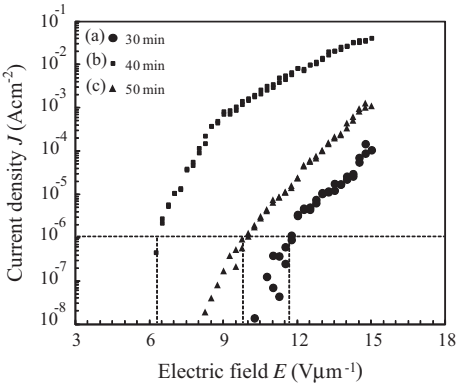

Fig. 4. The field emission characteristics of ZNs shown in Fig. 2, which were prepared at 300 °C for the growth period of (a) 30 min, (b) 40 min, and (c) 50 min respectively.

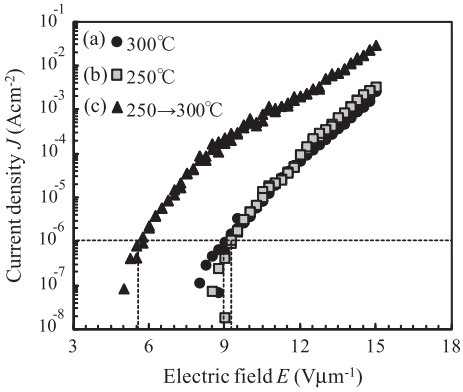

Fig. 5. The field emission characteristics of ZNs shown in Fig. 3, which were prepared at the growth temperatures of (a) 300 °C, (b) 250 °C, and (c) gradually increased from 250 °C to 300 °C during the growth period of 60 min respectively.

about 5.5 V/μm as shown in Fig. 5(c). This value is the lowest among the other samples with different growth temperature profiles. From the SEM images shown in Fig. 3, it is found that the average diameter of the tip of ZNs in the sample prepared at the constant growth temperature of 300 °C is about 100 nm, which is about 5 times to that of the sample prepared at 250 °C. In the case of the sample prepared at continuously varying temperatures between 250 °C and 300 °C as shown in Fig. 3(c), a relatively straight tip of ZNs with the average diameter of about 30 nm is achieved. There is also a difference in the structural appearance of the individual nanowire in the sample prepared at constant temperatures compared to that of the samples prepared at varying growth temperatures during the growth process. The latter exhibits a stiffer structure, i.e., the bending of nanowires is relatively small so that mutual interlacing of the nanowires, which could intense the screening effect on the emission electron, is reduced as shown in Fig. 3(c). In the former cases of constant temperatures, the bending of nanowires is quite obvious causing mutual interlacing of nanowires more often as shown in Fig. 3(a) and (b). Normally, it is expectable that the field emission will enhance when the sharpness (diameter) of the tip of ZNs emitter, which has similar average length and growth density, is increased (decreased). However, in comparing the morphology of the tips to the corresponding emission characteristic, the correlation between these parameters is not obvious in these samples. This could be due to the difference in the resistivity between these samples, which were prepared at different temperatures. In our USP technique, it is already known that the average diameter of the nanowires becomes smaller when prepared at lower growth temperatures [22–25]. On the other hand, the ZNs with higher resistance are achieved at lower temperatures. The average diameter and the sheet resistance of the corresponding samples are shown in Table 1. The sheet resistance of the sample prepared at the constant temperature of 250 °C is about 5.6×10^5 Ω/Square, which is about 7 times larger than that of the 300 °C. The increasing of sheet resistance could have counterbalanced the enhancement of aspect ratio due to decreasing of the average diameter of the tips so that the improvement in the field emission was compensated in this sample as sown in Fig. 5(b). It is also found that the sample prepared at the growth temperatures gradually varied from 250 °C to 300 °C during the growth period of 60 min exhibits a small average diameter of about 30 nm, which is close to that of the sample prepared at the constant temperature of 250 °C, while its sheet resistance is in the same order (about 8.5×10^4 Ω/Square) to that of the sample prepared at the constant temperature of 300 °C. Hence, the field emission characteristic of this sample is obviously enhanced due to both the benefits of improvement in aspect ratio (smaller tip average diameter) and lowering sheet resistance as shown in Fig. 5(c).

To investigate the effect of sheet resistance of the ZNs emitters, the field emission characteristics of the samples, which have different sheet resistances with similar morphology, are compared as shown in Fig. 6. It is observed that the sample with lower sheet resistance of about 9.2×10^2 Ω/Square, which is about two orders lower than the as-grown one having about 8.1×10^4 Ω/Square by annealing

Table 1
The average diameter and sheet resistance of the samples prepared at various temperature profiles.

Temperature profiles	Average diameter of the tips (nm)	Sheet resistance (Ω/Square)
300 °C	100	8.1×10^4
250 °C	20	5.6×10^5
250 → 300 °C	30	8.5×10^4
Post-annealing at 500 °C	100	9.2×10^2

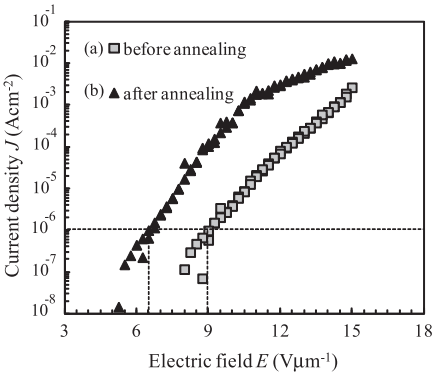

Fig. 6. The field emission characteristics of ZNs, which were prepared at the growth temperatures of 300 °C (a) without post-annealing process and (b) with post-annealing process at 500 °C for 10 min under vacuum of 10^{-4} Torr.

under the vacuum at 500 °C after the growth process of ZNs emitter, exhibits better emission with smaller threshold voltage of about 6.5 V/μm. When the sheet resistance is reduced to about two orders by post-annealing, improvement of the field emission current for about 10^2 times is achieved under the conditions of applied electric field below 11 V/μm as shown in Fig. 6(b). A gradual saturation of improvement observed at the applied electric fields higher than 11 V/μm could be due to the increasing of apparent resistance induced inside the nanowires by the impact of accelerating charges causing the lattice vibration and decreasing of apparent mobility. In these samples, only the self-assembled seeding layer with thickness less than 50 nm, the sheet resistance of which is relatively high, was utilized as the back electrode of the cathode. In order to reduce the sheet resistance of the whole cathode, an additional Mo back electrode, which was sputtered on the SLG substrate before the ZNs growth process, was applied. In Fig. 7, the result of field emission of this sample is shown in comparison with the one having similar morphology without the Mo back electrode. It is found that by adding the Mo back electrode, the threshold voltage is reduced to 7.2 V/μm, which is obviously lower than that of the sample without the additional back electrode as compared in Fig. 7(a) and (b). The results discussed above clearly indicate that lowering the sheet resistance of emitter itself as well as the back electrode could enhance the emission property. In Fig. 7(c), the field emission characteristic of the sample loaded with a 2 nm-thick Mo coated ZNs emitter is also shown in comparison. In this sample, the threshold voltage is reduced to about 7.7 V/μm and enhancement of emission current is also obtained. This enhancement could be due to the effect of lowering the tunneling barrier near the surface of ZNs by coating Mo, which has smaller work function than the ZnO, i.e., $\phi_{Mo} = 4.6$ eV < $\phi_{ZnO} = 5.3$ eV.

The corresponding F–N plots for the samples discussed above are shown in Fig. 8. It is found that all the plots exhibit a good linear dependency to the inverse of the applied electric field E, implying that the electron emission is governed by the tunneling mechanism explained by the Fowler–Nordheim expression as shown in the Eq. (1). In Table 2, the results of the corresponding field enhancement factors β deduced by equating the slopes of the plots in the Fig. 8 and the coefficient $(-B\phi^{3/2}/\beta)$ of the first term of the right hand side of Eq. (2), where $A = 1.56 \times 10^{-10}$ AV^{-2} eV, $B = 6.83 \times 10^9$ V eV$^{-3/2}$ μm^{-1}, and the corresponding work functions of the emitters such as $\phi_{ZnO} = 5.3$ eV or

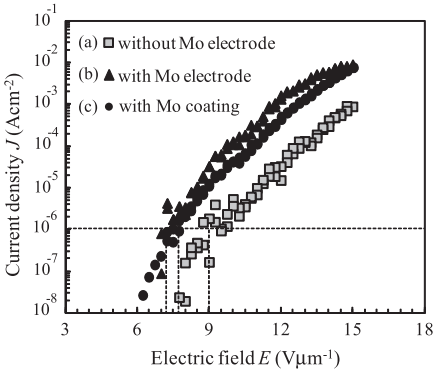

Fig. 7. The field emission characteristics of ZNs, which were prepared at the growth temperatures of 300 °C (a) without additional Mo back electrode, (b) with Mo back electrode, and (c) with ZNs emitter coated by 2 nm-thick Mo.

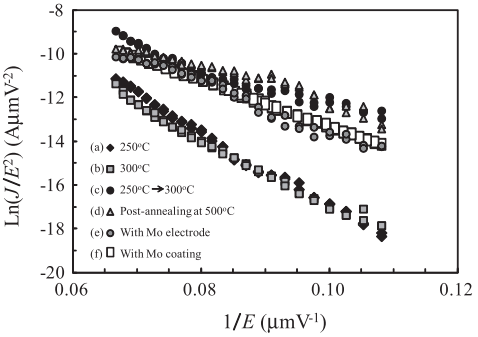

Fig. 8. The F–N plots for the samples prepared at the growth temperatures of (a) 250 °C, (b) 300 °C, (c) 250–300 °C range, (d) 300 °C with post-annealing process, (e) 300 °C with Mo back electrode, and (f) 300 °C with Mo coating.

Table 2
The field enhancement factors β and threshold voltages of the samples with various conditions of ZNs emitters.

Conditions of the samples	Field enhancement factor β	Threshold voltage (V/μm)
300 °C	544	9.0
250 °C	487	9.3
250 → 300 °C	953	5.5
Post-annealing at 500 °C	1068	6.5
With Mo electrode	737	7.2
With Mo coating	697	7.7

$\phi_{Mo} = 4.6$ eV were applied respectively. It is found that the β of the sample prepared at 250 °C, which has the highest sheet resistance and smallest average diameter of ZNs tips as shown in the Table 1, is the smallest compared to the others. It is also observed that the β of the sample prepared at 300 °C, which has larger average diameter of ZNs tips with lower sheet resistance, is relatively close to that of 250 °C. In the case of the sample prepared at the temperatures continuously varying from 250 °C to 300 °C, which has relatively small average diameter of ZNs tips and low sheet resistance, shows a value of β that is about twice to that of the sample prepared at constant temperature of 250 °C. The highest value of β is observed in the sample with post-annealing treatment, the sheet resistance of which is the lowest. By comparing the β to their corresponding threshold voltages as shown in the

Table 2, a good counter relation between these two parameters is observed, i.e., the larger the β, the lower is the threshold voltage of emission. It can be considered that the samples with higher aspect ratio as well as smaller sheet resistance would yield a better field enhancement factor resulting in the improvement of emission current. From these results, it can be said that the sheet resistance is also an important factor along with the aspect ratio of the emitter that could effect the emission property.

4. Conclusions

The field emission property of the ZnO nanowires emitters with various conditions fabricated by the ultrasonic spray pyrolysis was analyzed. Due to mutual interlacing phenomenon occurred between the lengthy nanowires, which behaved as a trade off mechanism against the benefit contributed by improvement of aspect ratio, an optimum average length of ZNs emitter to achieve high efficient field emission was existed. By comparing the field emission characteristics of the samples having different sheet resistances, it was found that the samples with smaller sheet resistance exhibited better field emission and low threshold voltage. It was also observed that utilization of additional Mo back electrode and coating of material with smaller work function such as Mo on the ZNs emitter could enhance the field emission property. The lowest threshold voltage of about 5.5 V/μm to obtained 1.0 μA/cm^2 was achieved in the sample prepared at the growth temperatures continuously varying from 250 °C to 300 °C during the growth process of ZNs, which has the average diameter of about 30 nm and the sheet resistance of about 8.5 × 10^4 Ω/Square. It was concluded that the average diameter of ZNs emitter and its sheet resistance were important factors that influent on the field emission property of ZNs prepared by this technique.

Acknowledgements

The authors would like to thank Mr. Isamu Minemura for his great help in setting up the experimental equipments.

References

[1] R.H. Fowler, L.W. Nordheim, Electron emission in intense electric fields, Proc. R. Soc. Lond., Ser. A 119 (1928) 173.
[2] C.J. Lee, T.J. Lee, S.C. Lyu, Y. Zhang, H. Ruh, H.J. Lee, Field emission from well-aligned zinc oxide nanowires grown at low temperature, Appl. Phys. Lett. 81 (2002) 3648.
[3] K.K. Naik, R. Khare, D. Chakravarty, M.A. More, R. Thapa, D.J. Late, C.S. Rout, Field emission properties of ZnO nanosheet arrays, Appl. Phys. Lett. 105 (2014) 233101.
[4] F.D. Nayeri, K. Narimani, M. Kolahdouz, E. Asl-Soleimani, F. Salehi, Surface structure optimization for cost effective field emission of zinc oxide nanorods on glass substrate, Thin Solid Films 571 (2014) 154.
[5] G. Zhang, L. Wei, Y. Chen, L. Mei, J. Jiao, Field emission property of ZnO nanoneedle arrays with different morphology, Mater. Lett. 96 (2013) 131.
[6] E. Mosquera, J. Bernal, R.A. Zarate, F. Mendoza, R.S. Katiyar, G. Morell, Growth and electron field-emission of single-crystalline ZnO nanowires, Mater. Lett. 93 (2013) 326.
[7] E. McCarthy, S. Garry, D. Byrne, E. McGlynn, J.-P. Mosnier, Field emission in ordered arrays of ZnO nanowires prepared by nanosphere lithography and extended Fowler–Nordheim analyses, J. Appl. Phys. 110 (2011) 124324.
[8] L.W. Chang, J.W. Yeh, C.L. Cheng, F.S. Shieu, H.C. Shih, Field emission and optical properties of Ga-doped ZnO nanowires synthesized via thermal evaporation, Appl. Surf. Sci. 257 (2011) 3145.
[9] F.J. Sheini, D.S. Joag, M.A. More, Electrochemical synthesis of Sn doped ZnO nanowires on zinc foil and their field emission studies, Thin Solid Films 519 (2010) 184.
[10] Z. Zhang, J. Huang, H. He, S. Lin, H. Tang, H. Lu, Z. Ye, The influence of morphologies and doping of nanostructured ZnO on the field emission behaviors, Solid-State Electron. 53 (2009) 578.
[11] J. Chen, W. Lei, W. Chai, Z. Zhang, C. Li, X. Zhang, High field emission enhancement of ZnO-nanorods via hydrothermal synthesis, Solid-State Electron. 52 (2008) 294.
[12] J. Xiao, Y. Wu, W. Zhang, X. Bai, L. Yu, S. Li, G. Zhang, Enhanced field emission from ZnO nanopencils by using pyramidal Si(100) substrates, Appl. Surf. Sci. 254 (2008) 5426.
[13] C.J. Park, D.-K. Choi, J.k. Yoo, G.-C. Yi, C.J. Lee, Enhanced field emission properties from well-aligned zinc oxide nanoneedles grown on the Au/Ti/n-Si substrate, Appl. Phys. Lett. 90 (2007) 083107.
[14] W. Wanga, G. Zhang, L. Yua, X. Baia, Z. Zhanga, X. Zhaoa, Field emission properties of zinc oxide nanowires fabricated by thermal evaporation, Physica E 36 (2007) 86.
[15] S.Y. Li, C.Y. Lee, P. Lin, T.Y. Tseng, Gate-controlled ZnO nanowires for field-emission device application, J. Vac. Sci. Technol. B 24 (2006) 147.
[16] Y. Zhang, K. Yu, S. Ouyang, Z. Zhu, Patterned growth and field emission of ZnO nanowires, Mater. Lett. 60 (2006) 522.

[17] Y.W. Zhu, H.Z. Zhang, X.C. Sun, S.Q. Feng, J. Xu, Q. Zhao, B. Xiang, R.M. Wang, D.P. Yu, Efficient field emission from ZnO nanoneedle arrays, Appl. Phys. Lett. 83 (2003) 144.
[18] C.X. Xu, X.W. Sun, Field emission from zinc oxide nanopins, Appl. Phys. Lett. 83 (2003) 3806.
[19] S.H. Jo, J.Y. Lao, Z.F. Ren, R.A. Farrer, T. Baldacchini, J.T. Fourkas, Field-emission studies on thin films of zinc oxide nanowires, Appl. Phys. Lett. 83 (2003) 4821.
[20] G. Sigircik, O. Erken, T. Tuken, C. Gumus, O.M. Ozkendir, Y. Ufuktepe, Electrosynthesis of ZnO nanorods and nanotowers: morphology and X-ray absorption near edge spectroscopy studies, Appl. Surf. Sci. 340 (2015) 1.
[21] Y. Zhang, M. Liu, W. Ren, Z.-G. Ye, Well-ordered ZnO nanotube arrays and networks grown by atomiclayer deposition, Appl. Surf. Sci. 340 (2015) 120.
[22] M.T. Htay, Y. Tani, Y. Hashimoto, K. Ito, Synthesis of optical quality ZnO nanowires utilizing ultrasonic spray pyrolysis, J. Mater. Sci. Mater. Electron. 20 (2009) 341.
[23] M.T. Htay, Y. Hashimoto, N. Momose, K. Ito, Position-selective growth of ZnO nanowires by ultrasonic spray pyrolysis, J. Cryst. Growth 311 (2009) 4499.
[24] M.T. Htay, M. Itoh, Y. Hashimoto, K. Ito, Photoluminescence properties and morphologies of submicron-sized ZnO crystals prepared by ultrasonic spray pyrolysis, Jpn. J. Appl. Phys. 47 (2008) 541.
[25] M.T. Htay, Y. Hashimoto, K. Ito, Growth of ZnO submicron single-crystalline platelets, wires, and rods by ultrasonic spray pyrolysis, Jpn. J. Appl. Phys. 46 (2007) 440.
[26] J.B.K. Law, C.B. Boothroyd, J.T.L. Thong, Site-specific growth of ZnO nanowires from patterned Zn via compatible semiconductor processing, J. Cryst. Growth 310 (2008) 2485.
[27] R.Q. Guo, J. Nishimura, M. Matsumoto, D. Nakamura, T. Okada, Catalyst-free synthesis of vertically-aligned ZnO nanowires by nanoparticle-assisted pulsed laser deposition, Appl. Phys. A: Mater. Sci. Process. 93 (2008) 843.
[28] H.L. Zhou, A. Chen, L.K. Jian, K.F. Ooi, G.K.L. Goh, K.Y. Zang, S.J. Chua, Template-directed selective growth of ordered ZnO nanostructures on GaN by the hydrothermal method, J. Cryst. Growth 310 (2008) 3626.
[29] R. Nishimura, T. Sakano, T. Okato, T. Saiki, M. Obara, Catalyst-free growth of high-quality ZnO nanorods on Si(100) substrate by two-step, off-axis pulsed-laser deposition, Jpn. J. Appl. Phys. 47 (2008) 4799.
[30] H.F. Shao, X.F. Qian, B.C. Huang, Novel growth of ZnO micro-rod arrays using hydrophobically micropatterned surfaces, Mater. Sci. Semicond. Process. 10 (2007) 68.
[31] W.Q. Yang, L. Dai, L.P. You, B.R. Zhang, B. Shen, G.G. Qin, Catalyst-free synthesis of well-aligned ZnO nanowires on $In_{0.2}Ga_{0.8}N$, GaN, and $Al_{0.25}Ga_{0.75}N$ substrates, J. Nanosci. Nanotechnol. 6 (2006) 3780.
[32] H. Ham, G.Z. Shen, J.H. Cho, T.J. Lee, S.H. Seo, C.J. Lee, Vertically aligned ZnO nanowires produced by a catalyst-free thermal evaporation method and their field emission properties, Chem. Phys. Lett. 404 (2005) 69.
[33] H.J. Fan, F. Fleischer, W. Lee, K. Nielsch, R. Scholz, M. Zacharias, U. Gösele, A. Dadgar, A. Krost, Patterned growth of aligned ZnO nanorod arrays on sapphire and GaN layers, Superlatt. Microstruct. 36 (2004) 95.
[34] Z.R. Tian, J.A. Voigt, J. Liu, B. Mckenzie, M.J. Mcdermott, M.A. Rodriguez, H. Konishi, H. Xu, Catalytic growth of zinc oxide nanowires by vapor transport, Nat. Mater. 2 (2003) 821.
[35] S.C. Liu, J.J. Wu, Low-temperature and catalyst-free synthesis of well-aligned ZnO nanorods on Si(100), J. Mater. Chem. 12 (2002) 3125.
[36] Y. Wu, H. Yan, M. Huang, B. Messer, J.H. Song, P. Yang, Inorganic semiconductor nanowires: rational growth, assembly, and novel properties, Chem. Eur. J. 8 (2002) 1260.
[37] M.H. Huang, Y. Wu, H. Feick, N. Tran, E. Weber, P. Yang, Catalytic growth of zinc oxide nanowires by vapor transport, Adv. Mater. 13 (2001) 113.
[38] Y. Li, G.W. Meng, L.D. Zhang, F. Phillipp, Ordered semiconductor ZnO nanowire arrays and their photoluminescence properties, Appl. Phys. Lett. 76 (2000) 2011.
[39] M.T. Htay, M. Okamura, R. Yoshizawa, Y. Hashimoto, K. Ito, Synthesis of a cuprite thin film by oxidation of a Cu metal precursor utilizing ultrasonically generated water vapor, Thin Solid Films 556 (2014) 211.